DOT/FAA/CT-84/14

Quasi-Steady Analysis of Aircraft Panel Flammability

Thor I. Eklund

June 1984

Final Report

U.S. Department of Transportation
Federal Aviation Administration
Technical Center
Atlantic City Airport, N.J. 08405

Technical Report Documentation Page

1. Report No.	2. Government Accession No.	3. Recipient's Catalog No.
DOT/FAA/CT-84/14		

4. Title and Subtitle	5. Report Date
QUASI-STEADY ANALYSIS OF AIRCRAFT PANEL FLAMMABILITY	June 1984
	6. Performing Organization Code ACT-350
	8. Performing Organization Report No. DOT/FAA/CT-84/14
7. Author(s) Thor I. Eklund	
9. Performing Organization Name and Address Federal Aviation Administration Technical Center Atlantic City Airport, New Jersey 08405	10. Work Unit No. (TRAIS)
	11. Contract or Grant No.
	13. Type of Report and Period Covered Final April 1983 - April 1984
12. Sponsoring Agency Name and Address U.S. Department of Transportation Federal Aviation Administration Technical Center Atlantic City Airport, New Jersey 08405	14. Sponsoring Agency Code

15. Supplementary Notes

16. Abstract

The purpose of this analysis is the development of a model that relates polymeric material properties to ignitability. The model is developed for an idealized fire test for ignitability of large-scale aircraft honeycomb panels in a vertical orientation.

Transport relations for radiative heat transmission and turbulent mass and energy transfer are applied to an idealized piloted ignition of a vertical aircraft panel. The incident radiative energy required for panel ignition is related to thermal decomposition temperatures from thermogravimetric analysis. Effects of pyrolysis energy requirements and temperature dependence of flammability lean limits are incorporated in the analysis. The analysis is quasi-steady, in that transient effects are ignored and a slow ramp heating of the panel is assumed. State-of-the-art panel materials are dominated by radiative effects at the point of ignition. The analysis demonstrates that higher polymer degradation temperatures result in improved fire-worthiness, that surface emissivities and reflectivities are the dominant factors controlling the incident radiation needed for ignition, and that the heat of pyrolysis becomes less significant in the energy balance as the polymer degradation temperature is raised.

17. Key Words	18. Distribution Statement
Aircraft Material Flammability Polymer Heat Transfer Ignition	Document is available to the U.S. public through the National Technical Information Service, Springfield, Virginia 22161

19. Security Classif. (of this report)	20. Security Classif. (of this page)	21. No. of Pages	22. Price
Unclassified	Unclassified	21	

Form DOT F 1700.7 (8-72) Reproduction of completed page authorized

METRIC CONVERSION FACTORS

Approximate Conversions to Metric Measures

Symbol	When You Know	Multiply by	To Find	Symbol
	LENGTH			
in	inches	*2.5	centimeters	cm
ft	feet	30	centimeters	cm
yd	yards	0.9	meters	m
mi	miles	1.6	kilometers	km
	AREA			
in^2	square inches	6.5	square centimeters	cm^2
ft^2	square feet	0.09	square meters	m^2
yd^2	square yards	0.8	square meters	m^2
mi^2	square miles	2.6	square kilometers	km^2
	acres	0.4	hectares	ha
	MASS (weight)			
oz	ounces	28	grams	g
lb	pounds	0.45	kilograms	kg
	short tons (2000 lb)	0.9	tonnes	t
	VOLUME			
tsp	teaspoons	5	milliliters	ml
Tbsp	tablespoons	15	milliliters	ml
fl oz	fluid ounces	30	milliliters	ml
c	cups	0.24	liters	l
pt	pints	0.47	liters	l
qt	quarts	0.95	liters	l
gal	gallons	3.8	liters	l
ft^3	cubic feet	0.03	cubic meters	m^3
yd^3	cubic yards	0.76	cubic meters	m^3
	TEMPERATURE (exact)			
°F	Fahrenheit temperature	5/9 (after subtracting 32)	Celsius temperature	°C

*1 in = 2.54 (exactly). For other exact conversions and more detailed tables, see NBS Misc. Publ. 286, Units of Weights and Measures, Price $2.25, SD Catalog No. C13.10:286.

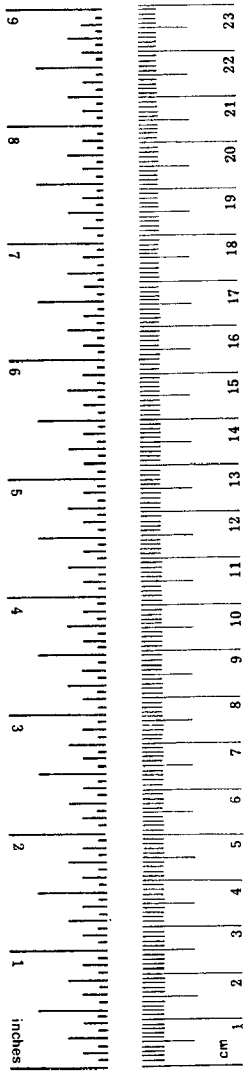

Approximate Conversions from Metric Measures

Symbol	When You Know	Multiply by	To Find	Symbol
	LENGTH			
mm	millimeters	0.04	inches	in
cm	centimeters	0.4	inches	in
m	meters	3.3	feet	ft
m	meters	1.1	yards	yd
km	kilometers	0.6	miles	mi
	AREA			
cm^2	square centimeters	0.16	square inches	in^2
m^2	square meters	1.2	square yards	yd^2
km^2	square kilometers	0.4	square miles	mi^2
ha	hectares (10,000 m^2)	2.5	acres	
	MASS (weight)			
g	grams	0.035	ounces	oz
kg	kilograms	2.2	pounds	lb
t	tonnes (1000 kg)	1.1	short tons	
	VOLUME			
ml	milliliters	0.03	fluid ounces	fl oz
l	liters	2.1	pints	pt
l	liters	1.06	quarts	qt
l	liters	0.26	gallons	gal
m^3	cubic meters	35	cubic feet	ft^3
m^3	cubic meters	1.3	cubic yards	yd^3
	TEMPERATURE (exact)			
°C	Celsius temperature	9/5 (then add 32)	Fahrenheit temperature	°F

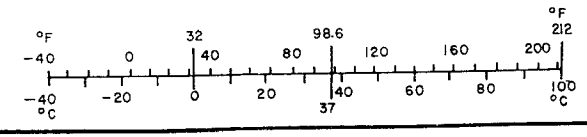

TABLE OF CONTENTS

	Page
EXECUTIVE SUMMARY	v
INTRODUCTION	1
Purpose	1
Background	1
Objective	1
ANALYSIS	2
Case Description	2
The Turbulent Boundary Layer	3
Energy Balance	7
Calculations	8
DISCUSSION	12
CONCLUSIONS	14
REFERENCES	14
APPENDICES	
A - Conduction Heat Transfer	
B - Thermogravimetric Analysis (TGA)	

LIST OF ILLUSTRATIONS

Figure		Page
1	Idealized Test Configuration	3
2	Typical Thermogram	4
3	Turbulent Boundary Layer	4
4	Ignition Heat Flux	10

LIST OF TABLES

Table		Page
1	Value of Terms	11
2	Pyrolysis Temperature and Net Heat Fluxes (T_p from Appendix B)	13

EXECUTIVE SUMMARY

Improved fire safety characteristics of aircraft interior materials can be obtained from a combination of lowered flame spread rate, lowered heat release rate, and more stringent ignition characteristics. The latter is of significance because preventing ignition will automatically bring the flame spread and heat release rates to zero.

In a postcrash fire scenario, aircraft sidewall panels and dividers are potentially exposed to large radiative heat flux from external fuel fires and burning materials within the fuselage. When exposed to such radiant heat, the panel's rise in temperature will be counterbalanced by convective heat transfer to the adjacent air as well as by emission and reflection of radiant heat by the panel surface.

This analysis relates heat and mass transfer processes to basic thermochemical properties of typical aircraft panel materials to develop piloted ignition criteria. The analysis demonstrates what magnitude imposed radiant heat flux is needed for ignition of a given polymer. Conversely, the analysis shows what panel thermochemical properties are required to prevent ignition for a range of imposed heat fluxes.

The analysis provides a technical framework for selection of polymeric materials that could resist ignition under specified radiative exposures.

INTRODUCTION

PURPOSE.

The purpose of this analysis is the development of a model that relates polymeric material properties to ignitability. The model is developed for an idealized fire test for ignitability of large-scale aircraft honeycomb panels in a vertical orientation.

BACKGROUND.

Aircraft sidewall panels are resistant to ignition from small energy sources as evidenced by the requirement to pass a flammability test specified in FAR 25.853(a). Nevertheless, a multitude of documented test programs (references 1, 2, 3, 4, and 5) have conclusively demonstrated that aircraft panels can burn in a realistic fire scenario. These test results are in keeping with fleet experience where aircraft have been destroyed from ramp fires, in-flight fires, and postcrash fires.

The reason that self-extinguishing panels can burn in an aircraft is the change in material exposure conditions. The process of burning involves evolution of flammable gases from a material surface with subsequent chemical reaction with oxygen from the surrounding air. Heat feedback from this gas phase combustion to the material must be adequate to continue the evolution of flammable gases. Otherwise, the combustion region becomes starved of fuel and the fire stops.

Most polymeric material systems require more heat to evolve flammable gases than their own flame is able to provide them. That is why they are self-extinguishing. However, they can burn when they get additional heat from nearby burning materials or from a strong radiant source such as a large fuel fire.

Thus, more severe flammability tests involve subjecting the material sample to some prescribed heat flux from an external source. Such tests are devised to measure such diverse flammability indicators as heat release rate, flame spread rate, mass loss or gas injection rate, and time for ignition. Nevertheless, these indicators will be affected by the external heat flux imposed in a particular test. If such a test were to be used for screening of materials, the external radiant heat flux would play a major role in determining what polymeric material systems could successfully pass the screening. Therefore, there are cogent reasons for studying the relation of radiant heat flux to ignitability of polymeric systems from a more fundamental point of view.

OBJECTIVE.

The objective of the analysis is the determination of the radiant heat fluxes required for ignition of a given polymeric system, and thereby, derive a relationship between the thermochemical properties of the polymer and the ignitability.

ANALYSIS

CASE DESCRIPTION.

Figure 1 shows an idealized simple test setup.* Radiant heat is externally applied to one side of an aircraft panel. Some of this applied heat flux is reradiated and reflected from the panel. Some of the heat is transferred to a buoyant boundary layer of air on each side of the panel. If degradation of the panel constituents is occurring, some heat may be absorbed in endothermic material processes. The analysis of the test setup is quasi-steady, in that, a slow ramp-type growth in heat flux is assumed. Another way to describe this approach is that the analysis is done for the lowest applied heat flux that could result in piloted ignition of a panel after a warmup period of many minutes. In this manner, transient conduction effects in the panel interior can be neglected, and the analysis can be done with steady-state equations. The analysis is developed to relate the applied heat flux to panel flammability. When enough heat is applied to the panel, the surface temperature will reach a state where the polymeric contents can degrade and outgas flammable species. The analysis includes the relationship of the concentration of these species to the lean limit of flammability.

The overall energy balance for figure 1 can be written as follows:

$$q_{NET}\, A = \frac{k}{\delta}\,(T-T_B)\, A + hA\,(T-T_o) + \dot{m}\, L_p\, A \qquad (1)$$

where A is the panel surface area on each side, q_{NET} is net radiant heat flux absorbed by the panel, k is the panel conductivity, δ is the panel thickness, T is the panel surface temperature on the irradiated side, T_B is the panel backside temperature, h is the convective heat transfer coefficient, T_o is the ambient temperature, $\dot{m}$ is the panel mass loss rate, and L_p is the panel heat of gasification per unit weight. If the panel is relatively thin, and the heating is slow, the panel will be assumed to be thermally thin within the context of the analysis in order to develop a first approximation. This means that the temperature is uniform across the panel cross-section and that the radiative and convective heat losses from the panel will be identical on each surface. This approximation will be examined further as to accuracy (appendix A).

Thus equation 1 can be written as

$$q_{NET} = 2\, h\,(T-T_o) + \dot{m}\, L_p + 2q_p \qquad (2)$$

and the net radiant flux can be further defined as

$$q_{NET} = q_{INC} - q_{REF} \qquad (3)$$

where q_{INC} is the incident flux to the heated surface, and $2q_p$ is the radiation emitted from the panel itself, and q_{REF} is the incident heat flux reflected by the panel surface.

Equations 1, 2, and 3 will be developed in such a manner that when the panel temperature meets the polymer decomposition temperature, T_p, a heat balance will be set up with the following characteristics. The material is exposed to a certain heat flux. The surplus incident heat flux over that lost by convection and radiation from the panel must be adequate to cause enough pyrolysis to form a flammable fuel air mixture in the panel boundary layer.

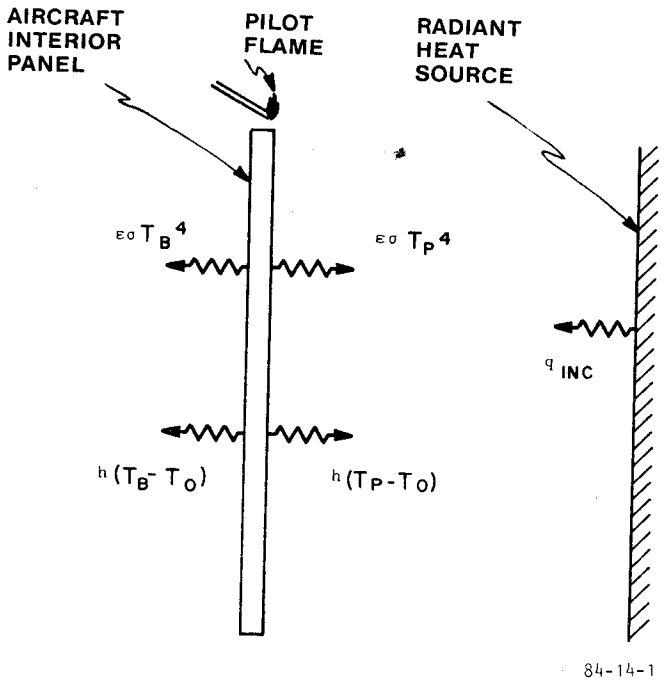

FIGURE 1. IDEALIZED TEST CONFIGURATION

Because the analysis is for large buoyancy forces and large temperature gradients, the boundary layer can be shown to be turbulent. Application of this analysis to smaller laboratory tests might involve slight modification to the test so that the laminar boundary layer is tripped.

The actual polymer decomposition temperature to be used in this type analysis needs some elaboration. A typical thermogram of a polymer of the type used in an aircraft panel is shown in figure 2. Such thermograms are relatively common data outputs from thermogravimetric analysis. Generally, the majority of the weight loss occurs within a relatively small temperature range of the order of 100 centigrade degrees, though there are a few exceptions to this. For the purpose of this analysis, T_p might be chosen as the point of ten percent weight loss, the point of steepest weight loss, or the point where the weight loss is half the total weight loss. For this analysis, the latter definition will be used as illustrated in figure 2. The literature on thermogravimetric analysis and differential scanning calorimetry is also useful in obtaining the heat of pyrolysis, L_p, for this analysis.

THE TURBULENT BOUNDARY LAYER.

The turbulent boundary layer must be characterized both for heat loss from the panel and for fuel air ratio. Figure 3 shows the type of temperature, velocity, and fuel concentration ratios that might arise from a heated polymeric vertical panel. In many boundary layer problems, the mass transfer is related to the velocity profile through a Reynolds analogy approach. However, because a natural ventilation boundary layer has a peak velocity (hence, zero velocity gradient) within it, a more traditional approach would result in zero mass transfer at the velocity peak. To circumvent this problem, the mass transfer will be tied to empirical relations that describe the heat transfer from vertical surfaces.

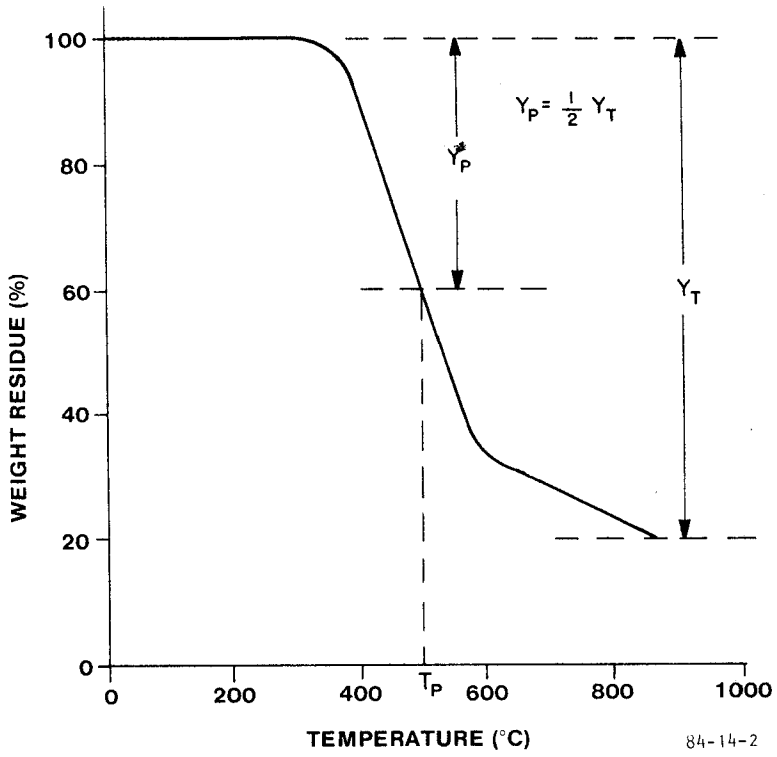

FIGURE 2. TYPICAL THERMOGRAM

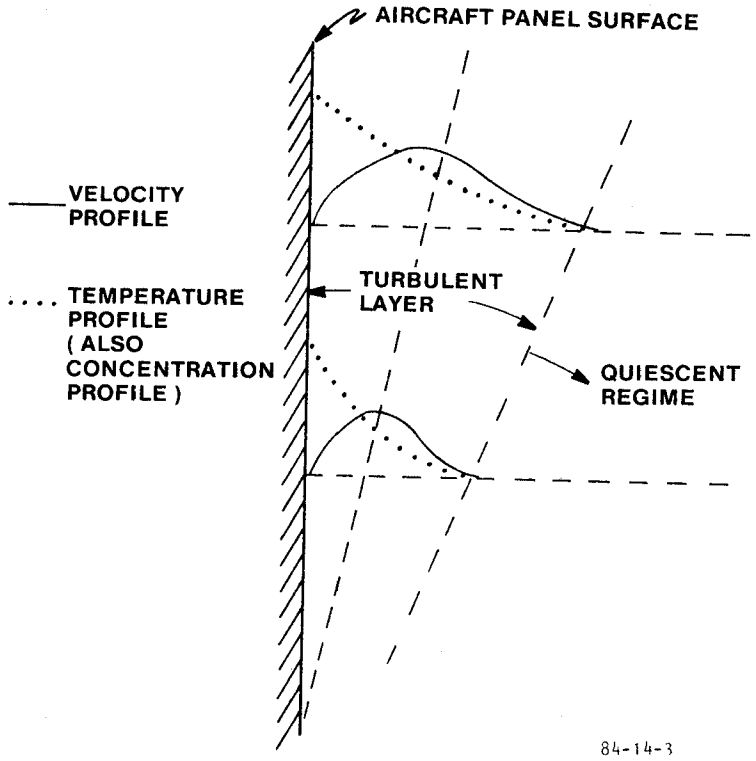

FIGURE 3. TURBULENT BOUNDARY LAYER

The following heat transfer relationship from reference 6 will be used

$$h = \frac{k_g}{L} (0.13) (Gr\ Pr)^{1/3} \tag{4}$$

where h is the convective heat transfer coefficient, k_g is the gas phase thermal conductivity, L is the height of the vertical panel, Gr is the Grashof number, and Pr is the Prandtl number. In reference 6, the experimental observation is stated that for turbulent boundary layers on heated vertical panels, the heat transfer per unit area is independent of height. This observation suggests that the pyrolysis rate will also be invariant with height.

The analogy between heat and mass transfer will be developed in the following way using the nomenclature from reference 7. The approach is simplified in that the relations are for diffusion of a single fuel specie through air. The turbulent diffusion of a fuel specie through the turbulent boundary layer is given as

$$\bar{J}_{Ay}(t) = - l^2 \left|\frac{d\bar{v}_x}{dy}\right| \frac{d\bar{C}_A}{dy} \tag{5}$$

where $\bar{J}_{Ay}(t)$ is the molar flux, $\bar{C}_A$ is the molar concentration, l is the turbulent mixing length, and v_x is the mean velocity parallel to the wall at a given distance y from from the wall. Similarly, the diffusion of heat is given by

$$\bar{q}_y(t) = - \rho\ C_p\ l^2 \left|\frac{d\bar{v}_x}{dy}\right| \frac{d\bar{T}}{dy} \tag{6}$$

where $q_y(t)$ is the heat transfer per unit area, ρ is the gas phase density, C_p is the gas phase specific heat, and T is the mean gas temperature at a given distance y from the wall. Combining equation 5 and equation 6 allows the mixing length and velocity gradient to cancel out.

$$\frac{\bar{J}_{Ay}(t)}{q_y(t)/\rho C_p} = \frac{\frac{d\bar{C}_A}{dy}}{\frac{d\bar{T}}{dy}} \tag{7}$$

Equation 7 can be rearranged and the term replaced by terms from the perfect gas law to get

$$\frac{p}{RT} C_p\ dT \frac{\bar{J}_{Ay}(t)}{q_y(t)} = d\bar{C}_A \tag{8}$$

Equation 8 can be integrated from the wall to infinity to get

$$\bar{C}_A\Big|_w = \frac{\bar{J}_{Ay}(t)}{\bar{q}_y(t)} \frac{p\ C_p}{R} \left[\ln \frac{\bar{T}_w}{\bar{T}_\infty}\right] \tag{9}$$

During pyrolysis $\overline{J}_{Ay}^{(t)}$ is the mass loss rate of the panel divided by the average molecular weight of the outgasing species and $\overline{q}_y^{(t)}$ is known from equation 4. Thus, equation 9 can be written as

$$\overline{C}_A\Big|_w = \frac{\dot{m}}{M} \frac{L}{k_g\ (0.13)\ (Gr\ Pr)^{1/3}\ (\overline{T}_w - \overline{T}_\infty)} \frac{p\ C_p}{R} \left[\ln\left(\frac{\overline{T}_w}{\overline{T}_\infty}\right)\right] \qquad (10)$$

Thus, a turbulent analogy between heat and mass transfer allows the flammable specie concentration at the wall to be stated in terms of the empirically known heat transfer rate. The significance of equation 10 is further that $\overline{C}_A\Big|_w$ must be raised to the lean limit concentration for the wall to be ignited by a pilot flame. Furthermore, in this analysis $\overline{T}_w$ will be taken as the pyrolysis temperature T_p and $\overline{T}_\infty$ will be taken as the ambient temperature T_0.

On a mass basis, the fuel air ratio is written

$$\frac{f}{a} = \frac{M\ \overline{C}_A}{\rho} \qquad (11)$$

or the mean specie molecular weight times the specie molar concentration divided by the density of air. At the wall, the air density can be written as

$$\rho = \frac{p}{RT_p} \qquad (12)$$

so that equation 10 can be used to write the fuel air ratio at the wall

$$\frac{f}{a} = \dot{m}\ \frac{L\ C_p\ T_p}{k_g\ (0.13)\ (Gr\ Pr)^{1/3}\ (T_p - T_o)} \left[\ln\left(\frac{T_p}{T_o}\right)\right] \qquad (13)$$

Now the lean limit for many hydrocarbons at 25° C is in the neighborhood of 45 milligrams per liter. However, the lean limit is sensitive to temperature. From reference 8, the following expression might be used to typify lean limit variation with temperature on a volumetric basis in terms of degrees centigrade

$$L_t = L_{25°}\left[1 - 0.000721\ (T-25°)\right] \qquad (14)$$

This can be rewritten on a mass basis for standard atmospheric pressure as

$$\frac{f}{a} = \frac{45}{1184}\left[1 - 0.000721\ (T-25°)\right] \qquad (15)$$

Thus, equation 15 can be related to equation 13 to show when the lean limit will be reached.

$$\frac{45}{1184}\left[1 - 0.000721\ (T_p - 298°\ K)\right] = \dot{m}\ \frac{L\ C_p\ T_p}{k_g\ (0.13)\ (Gr\ Pr)^{1/3}\ (T_p - T_o)} \left[\ln\left(\frac{T_p}{T_o}\right)\right] \qquad (16)$$

Although the Grashof number is temperature sensitive, the terms in equation 16 are specified by the pyrolysis temperature, thermal conductivity, Prandtl number, and ambient temperature. Use of the turbulent analogy leads to an explicit relationship yielding the mass loss rate of the panel required for piloted ignition. A simple rearrangement of equation 16 shows this more clearly.

$$\dot{m} = \frac{k_g\ (0.13)\ (Gr\ Pr)^{1/3}\ (T_p - T_o)}{L\ C_p\ T_p\ \ln\left[\left(\frac{T_p}{T_o}\right)\right]} \quad \frac{45}{1184}\ \left[1 - 0.000721\ (T_p - 298°K)\right]$$

Equation 17 is the critical building block for finding the required heat flux for piloted ignition. The factor 45/1184 will be carried explicitly in the analysis because a more accurate lean limit parameter could be chosen if the outgasing species of a given polymer were specificaly known.

ENERGY BALANCE.

Equation 17 relates the mass flux from the surface to the fuel air concentration needed for piloted ignition. To generate this required mass flux, there must be enough heat input to the material to pyrolyze the material at the appropriate decomposition temperature according to equation 2. Using equations 2 and 4, the mass loss rate can be written as

$$\dot{m} = \frac{q_{NET}}{L_p} - \frac{2k_g}{LL_p}\ (T_p - T_o)\ (0.13)\ (Gr\ Pr)^{1/3} - \frac{2q_p}{L_p} \qquad (18)$$

This is for the case where within the context of the problem, the panel is considered uniform in temperature. A more complex approach would involve non-uniform temperature distribution in the panel, in which case equation 18 would be rewritten as

$$\dot{m} = \frac{q_{NET}}{L_p} - \frac{k_g}{LL_p}\ (T_p - T_o)\ (0.13)\ (Gr\ Pr)^{1/3} - \frac{k}{\delta L_p}\ (T_p - T_B) - \frac{q_p}{L_p} - \frac{q_B}{L_p} \qquad (19)$$

where k is the thermal conductivity of the panel, δ is the panel thickness, and T_B is the panel backface temperature. Equating equation 18 to equation 17 leads to

$$q_{NET} = 2q_p + \frac{k_g}{L}\ (T_p - T_o)\ (0.13)\ (Gr\ Pr)^{1/3} \left\{ 2 + \frac{\frac{45}{1184}\ L_p}{C_p\ T_p\ \ln\ (T_p/T_o)}\ \left[1 - 0.000721\ (T_p - 298°K)\right] \right\} \qquad (20)$$

The left side of equation 20 is the net heat absorbed by the panel. The right hand side of equation 20 includes the radiation emitted from the panel surface and this term is explicitly written as follows:

$$q_p = \varepsilon \sigma T_p^4 \tag{21}$$

where is the emissivity of the panel surface and is the Sefan-Boltzmann constant. Combining equation 20 and 21 allows definition of the heat flux from an external source needed for piloted ignition of a panel with pyrolysis temperature T_p.

$$q_{NET} = 2 \varepsilon \sigma T_p^4 + \frac{k_g}{L} (T_p - T_o) (0.13) (Gr\ Pr)^{1/3} \left\{ 2 + \frac{\frac{45}{1184} L_p}{C_p T_p \ln (T_p/T_o)} \left[1 - 0.000721 (T_p - 298°K)\right] \right\} \tag{22}$$

For the purpose of this analysis, will be taken as 0.7. However, information on at pyrolysis temperatures for polymeric systems is scarce. It should also be noted that in real test apparatuses, as the specimen heats up and provides feedback to the external heat source, that heat source may get hotter and increase the incident levels to the specimen. This analysis assumes that the external heat source is controlled so that the incident heat to the test sample is accurately known.

CALCULATIONS.

Use of equation 22 to calculate the external heat flux required to allow piloted ignition is predicated on the knowledge of the Grashof-Prandtl number grouping as a function of temperature as well as knowledge of the gas conductivity, specific heat, and the heat of pyrolysis. The total expression for heat transfer per unit area is given by

$$q = \frac{k_g}{L} (0.13) (Gr\ Pr)^{1/3} (T_p - T_o) \tag{23}$$

where

$$(Gr\ Pr)^{1/3} = \left[\frac{C_p\ \rho^2 g\ \beta (T_p - T_o) L^3}{\mu k_g} \right]^{1/3} \tag{24}$$

where ρ is the air density, g is the gravitational constant, β is the expansion coefficient, and μ is the viscosity. The various properties that are temperature dependent will be selected at the middle temperature of $(T_p + T_o)/2$; which will be identified as T_m. The expansion coefficient β is simply $1/T_o$. From simple kinetic theory, the viscosity will be taken as

$$\mu = \mu_o \sqrt{\frac{T_m}{T_o}} \tag{25}$$

and the thermal conductivity will be taken as

$$k_g = k_{go} \sqrt{\frac{T_m}{T_o}} \tag{26}$$

From the perfect gas law, the density is simply

$$\rho = \frac{T_o}{T_m} \rho_o \tag{27}$$

Using equations 24, 25, 26, and 27, equation 23 can be written as

$$q = (0.13)\, k_o^{2/3}\, \rho_o^{2/3}\, T_o^{1/6} \left(\frac{C_p g}{\mu_o}\right)^{1/3} \frac{(T_p - T_o)^{4/3}}{\left(\frac{T_p + T_o}{2}\right)^{1/2}} \tag{28}$$

The actual values for use in equation 28 are as follows:

$k_o = 602 \times 10^{-7}$ cal cm^{-1} sec^{-1} $^oK^{-1}$

$\mu_o = 1851 \times 10^{-7}$ g cm^{-1} sec^{-1}

$C_p = 6.973$ cal $g\text{-mole}^{-1}$ $^oK^{-1}$

$\rho_o = 0.00121$ g cm^{-3}

With the use of these values, equation 28 can be written as

$$q = 0.0968 \times 10^{-2} \frac{(T_p - T_o)^{4/3}}{(T_p + T_o)^{1/2}} \tag{29}$$

where T_o is 293° K (20° C). With the use of equation 29, equation 22 is rewritten as

$$q_{NET} = 2\, \varepsilon \sigma T_p^4 + 0.0968 \times 10^{-2} \frac{(T_p - T_o)^{4/3}}{(T_p + T_o)^{1/2}} \left\{ 2 + \frac{\frac{45}{1184} L_p}{C_p T_p \ln\left(\frac{T_p}{T_o}\right)} \left[1 - 0.000\,721\,(T_p - 298)\right] \right. \tag{30}$$

With equation 30, all the terms needed to calculate q_{NET} are identified. The heat of pyrolysis will be taken as 200 cal/g although a number like 400 to 500 cal/g might be more common among aircraft panel components. The analysis will show that the panel flammability is not too sensitive to such changes in heat of pyrolysis. Table 1 shows the values of the terms in equation 30 along with q_{NET} as a function of T_p. On the right hand side of equation 30, the first term is the panel surface radiative loss, the second term is the wall turbulent convective heat loss, and the last term is the heat involved in pyrolyzing enough vapor for a flammable mixture. Figure 4 is a graph of the values found in table 1.

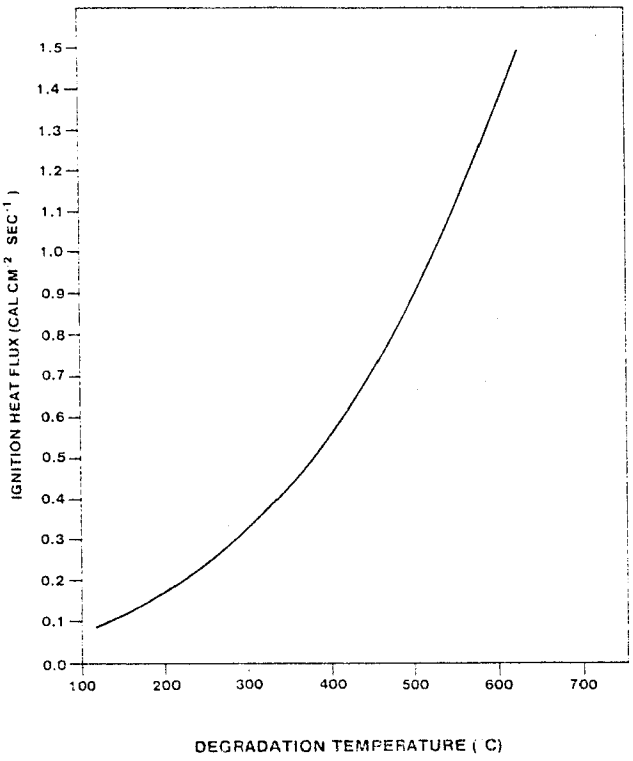

FIGURE 4. IGNITION HEAT FLUX

TABLE 1. VALUE OF TERMS

T_p (°K)	$2\epsilon\sigma T_p^4 \times 10^2$ (cal cm^{-2} sec^{-1})	$2\ q_t \times 10^2$ (cal cm^{-2} sec^{-1})	$q_v \times 10^2$ (cal cm^{-2} sec^{-1})	$2q_t + q_v$ (cal cm^{-2} sec^{-1})	q_{NET} (cal $sec^{-1} cm^{-2}$)	T_p (°C)
393	4.525	3.44	.658	.0400	.0853	120
418	5.791	4.54	.661	.0520	.1099	145
443	7.306	5.68	.658	.0634	.1365	170
468	9.100	6.86	.650	.0751	.1661	195
493	11.206	8.08	.641	.0872	.1993	220
518	13.658	9.30	.628	.0993	.2359	245
543	16.492	10.54	.613	.1115	.2764	270
568	19.745	11.80	.598	.1240	.3215	295
593	23.458	13.06	.582	.1364	.3710	320
618	27.671	14.34	.566	.1491	.4258	345
643	32.427	15.62	.550	.1617	.4860	370
668	37.772	16.88	.532	.1741	.5518	395
693	43.752	18.16	.515	.1868	.6243	420
718	50.416	19.46	.499	.1996	.7038	445
743	57.813	20.74	.482	.2122	.7903	470
768	65.993	22.04	.466	.2251	.8851	495
793	75.017	23.32	.450	.2377	.9879	520
818	84.934	24.60	.433	.2503	1.0996	545
843	95.863	25.88	.417	.2630	1.2210	570
868	107.683	27.16	.402	.2756	1.3524	595
893	120.635	28.44	.386	.2883	1.4947	620

DISCUSSION

The most salient features arising from equation 30 and table 1 are the importance of panel reradiation and pyrolysis temperature. In the overall energy balance, the energy required to generate the flammable fuel-air mixture through pyrolysis is much less than the energy needed to balance panel reradiation. This suggests that advanced fire resistant panels need a large T_p. In the analysis, reflectivity of the panel surface was implicitly treated with the radiant source term. Like the emissivity, the reflectivities at decomposition temperatures are not well known. Reference 9 uses values of emissivity and reflectivity of 0.87 to 0.72 and 0.15, respectively, for thermochemical analysis of an aircraft panel. In the case of the reflectivity, the incident heat flux is related to the previously defined absorbed heat flux by

$$q_{NET} = q_{INC} - \beta q_{INC} \tag{31}$$

or

$$q_{NET} = \alpha q_{INC} \tag{32}$$

where $\alpha = 1 - \beta$ and β is the reflectivity. A highly reflective surface would result in decreased ignitability. Further sophistication of this quasi-steady analysis would involve specific inclusion of the thermal conductivity of the panel. Appendix A addresses this complication.

The soundness of the overall analysis would best be assessed by comparisons with appropriate experimental data. Table 2 gives typical polymer degradation temperatures for materials used in current or proposed aircraft panels as well as the heat fluxes for piloted ignition from figure 4. The data in table 2 are taken from the thermograms in references 10, 11, and 12. One difficulty encountered in searching for appropriate flammability data is the fact that test materials are generally described generically (epoxy, phenolic, etc.) rather than by manufacturer specification number. As is evidenced in appendix B, large variations in decomposition behavior can be evidenced by different epoxies, different phenolics, etc.

Figure 4, in conjunction with table 2, leads to a significant conclusion. To withstand ignition under an imposed heat flux of 5 watts cm^{-2} or 1.19 cal cm^{-2} sec^{-1}, the polymer decomposition temperature must be at least 560° C. Only polyimide is clearly beyond this point. What figure 4 further shows is that the higher the polymer degradation temperature, the greater incremental improvement in flammability behavior will occur with a given increment in polymer decomposition temperature. This is due to the increased role of surface radiation at the higher specimen surface temperatures.

The significance of the 5-watt cm^{-2} type flux arises from documentation of heat flux from large external pool fires through fuselage openings as quantified in reference 13. Because the heat flux to the fuselage skin is approximately 15-watt cm^{-2}, large heat fluxes are involved in material exposures within the fuselage near the opening. Thus, test methods, that use lower fluxes like 2.5-watt cm^{-2}, really do not reflect the environment found in a postcrash fire.

TABLE 2. PYROLYSIS TEMPERATURES AND NET HEAT FLUXES (T_p FROM APPENDIX B)

Material	T_p (°C)	q_{NET} (w cm^{-2})
Epoxy		
Fiberite MXB-7203	500	3.8
Phenolic		
Narmco 8250	570	5.1
Ciba-Geigy Fibredux 917G	500	3.8
Fiberite MXB-6070	530	4.3
Fiberite MXT-6032	530	4.3
Bismaleimide		
Hexcel 531	550	4.7
Rhodia Kerimid 601	620	6.3
Vinylpolystyrlpyridine	560	4.9
Polyimide		
FN 308/7-11A	620	6.3
Dupont Pyralin 3062	620	6.3

This analysis addresses only panel ignitability. Two other flammability aspects, flame spread and heat release rate, are not included. While reference 14 shows empirical relationships between ignitability and flame spread, the total heat release of a panel at a given incident radiant flux is affected by other material parameters. These parameters may include the density of the panel, the volatile mass fraction, and the calorific values of the volatilized mass. The rate of heat release will also be affected by the panel conductivity and the growth of insulating char layers. Transient heat transfer effects will play an important role in the time history of the heat release rate.

What the quasi-steady analysis of aircraft panel flammability yields is a conservative approach for selecting panel materials for various locations as a function of anticipated fire exposure conditions. The approach is conservative because empirical studies like those described in reference 14 show that more and more heat flux is required for ignition as the material heating rate is increased. Thus, the quasi-steady analysis represents a worst case condition in this regard. That is, higher heat fluxes are needed to attain piloted ignition in shorter time.

The dominant role played by radiative heat transfer has some significant implications. The first has to do with char-forming type materials. While it has been correctly postulated that these materials offer improved heat release characteristics due to both decreased evolution of volatiles and growth of an insulating char layer, potential improvements in ignitability have been less obvious. However, if char development changes the material surface emissivity and absorptivity, piloted ignition could involve a different incident heat flux even if the degradation temperature remains unchanged. The other aspect of the dominance of radiation has to do with analyses of ignitability of horizontal or off-vertical surfaces. Because the convective heat transfer becomes such a small portion of the overall heat transfer during ignition of materials with high degradation temperatures (500° C and higher), the analysis developed here is probably applicable to a good

approximation, regardless of the material orientation. Thus, given a postulated radiant exposure for a given fire scenario, materials could be selected rationally based on thermal degradation characteristics.

Finally, it should be noted that the conductivity correction of appendix A results in a twenty-five percent lowering of the incident heat flux for ignition. Inclusion of the reflectivity explicitly in the analysis would raise the incident heat by twenty-five percent from the defined net absorbed heat if the reflectivity were twenty-percent. Thus, to some degree, these refinements counterbalance one another.

CONCLUSIONS

A quasi-steady analysis of aircraft panel flammability leads to an algebraic equation relating polymer degradation temperature to minimum applied heat flux for ignition. The analysis results in the following conclusions:

1. Use of panels with high polymer degradation temperatures improves fireworthiness.

2. Radiative heat transfer is the dominant energy transaction that controls the ignitability of state-of-the-art honeycomb panels.

3. The higher the polymer degradation temperature of a panel, the less significant is the heat of pyrolysis in flammability.

REFERENCES

1. Marcy, J. F., Air Transport Cabin Mockup Fire Experiments, FAA-RD-70-81, December 1970.

2. Marcy, J. F., A Study of Air Transport Passenger Cabin Fires and Materials, FAA-ADS-44, December 1965.

3. Sarkos, C. P., Hill, R. G., and Howell, W. D., The Development and Application of a Full-Scale Wide-Body Test Article to Study the Behavior of Interior Materials During a Postcrash Fuel Fire, AGARD-LS-123, May 1982.

4. Alpert, R. L., Pressure Modeling of Vertically Burning Aircraft Materials, FAA-RD-78-139, January 1979.

5. Sarkos, C. P., and Hill, R. G., Effectiveness of Seat Cushion Blocking Layer Materials against Cabin Fires, SAE PAPER 821484, 1982.

6. Kreith, F., Principles of Heat Transfer, Second Edition, International Textbook Company, Scranton, Pennsylvania, 1965.

7. Bird, R. B., Stewart, W. E., and Lightfoot, E. N., Transport Phenomena, John Wiley and Sons, Inc., New York, 1960.

8. Zabetakis, M. G., Flammability Characteristics of Combustible Gases and Vapors, United States Department of the Interior, Bulletin 627, 1965.

9. Ramohalli, K., Thermochemical Response of Honeycomb Sandwich Panels, J. of Fire Sciences, Volume I, pp. 379-395, September/October 1983.

10. Anderson, R. A., Arnold, D. B., and Johnson, G. A., Development of Aircraft Lavatory Compartments with Improved Fire Resistance Characteristics - Phase II, NASA CR-152120, February 1979.

11. Silverman, B., and Norris, F., Development of Processes and Techniques for Molding Thermally Stable, Fire-Retardant, Low-Smoke-Emitting Polymeric Materials, NASA Contract Report 151862, March 1979.

12. Hsu, M. S., Development of New and Improved Polymer Matrix Resin Systems (Phase I), HC Chem Research and Service Report No. 1001, NASA Ames Research Center Contract NAS 2-11529, December 1983.

13. Eklund, T. I., Pool Fire Radiation Through a Door in a Simulated Aircraft Fuselage, FAA-RD-78-135, December 1978.

14. Harkleroad, M., Quintiere, J., and Walton, W., Radiative Ignition and Opposed Flow Flame Spread Measurements on Materials, DOT/FAA/CT-/28, August 1983.

15. Eklund, T. I., Effects of Ventilation and Panel Properties on Temperature Rise from Aircraft Fires, DOT/FAA/CT-TN 83/63, January 1984.

APPENDIX A

CONDUCTION HEAT TRANSFER

To investigate the effects of wall conductivity on this analysis, the development of equation 22 must be modified to handle a backface temperature, T_B. In this manner, equation 22 becomes

$$q_{NET} = \varepsilon\sigma\left[T_p^4 + T_B^4\right] + \frac{k_g}{L}(T_B - T_o)(0.13)(Gr\ Pr)^{1/3}\Big|_B \qquad (A\text{-}1)$$

$$+ \frac{k_g}{L}(T_p - T_o)(0.13)(Gr\ Pr)^{1/3}\left\{1 + \frac{\frac{45}{1184}L_p}{C_p T_p \ln(T_p/T_o)}\left[1 - 0.000721(T_p - 298)\right]\right\}$$

The steady state heat conduction through the wall must be equal to the heat lost from the back wall by convection and radiation. This can written as follows:

$$\frac{k}{\delta}(T_p - T_B) = \varepsilon\sigma T_B^4 + \frac{k_g}{L}(T_B - T_o)(0.13)(Gr\ Pr)^{1/3}\Big|_B \qquad (A\text{-}2)$$

where k is the panel thermal conductivity and δ is the panel thickness. Although panel conductivities are not well established, the approach described in reference 15 could be used here. From this type analysis, a panel might be expected to have a thermal conductivity of 0.437 w/m °C. A typical panel might be nominally one-quarter inch thick. The right and left hand sides of equation A-2 can be plotted together as a function of T_B as is shown in figure A-1. The left running lines represent the panel conduction terms for various values of T_p. Where a straight line intersects the wall loss curve will identify the equilibrium backface temperature T_B. This intersection also marks the total heat output through the backface. The correction to the overall analysis can be demonstrated for the case of T_p equal to 500° C. On figure A-1, the intersection point is labeled K and this gives the actual heat transfer through the panel. If the conduction line is then dropped to point L and then moved up to point M, the heat transfer for the case of a uniform panel temperature is found. Because roughly half of the heat is lost through the backface, the overall change in q_{NET} is given by the following:

$$\frac{\Delta q_{NET}}{q_{NET}} = 1/2\left(1 - \frac{q_K}{q_M}\right) \qquad (A\text{-}3)$$

In this particular example, the fractional change comes out to 0.25. Thus, in this particular example, the absorbed heat flux required for long time ignition would actually be twenty-five percent less than that predicted by equation 30. This kind of correction process would get slightly more complicated if the panel had a backing layer of insulation.

Figure A-2 shows the effect of changes in panel thickness on the backface heat loss. A thinner panel would result in a smaller correction factor to the ignition heat flux predicted by equation 30.

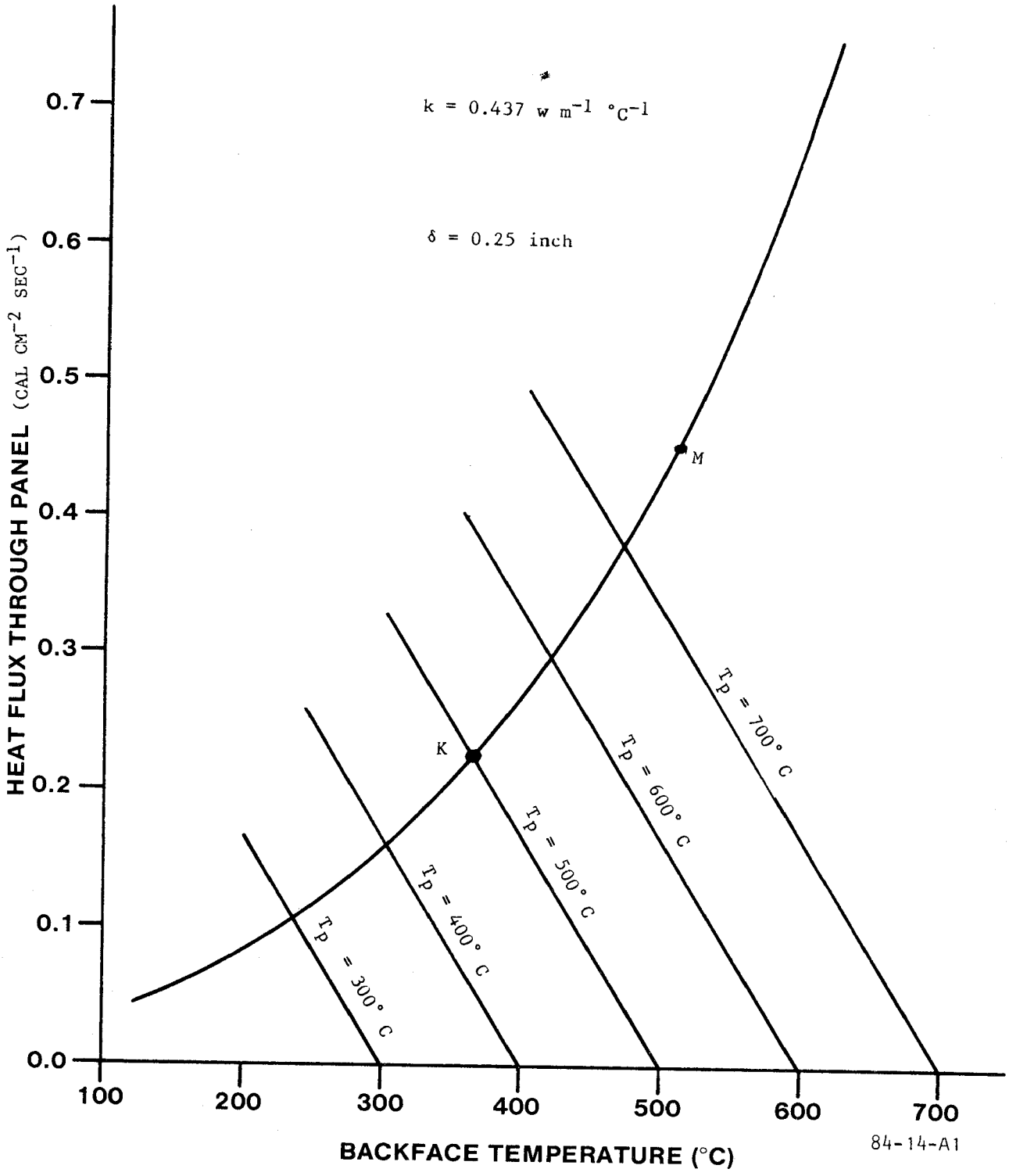

FIGURE A-1. EFFECT ON DEGRADATION TEMPERATURE ON PANEL HEAT TRANSFER

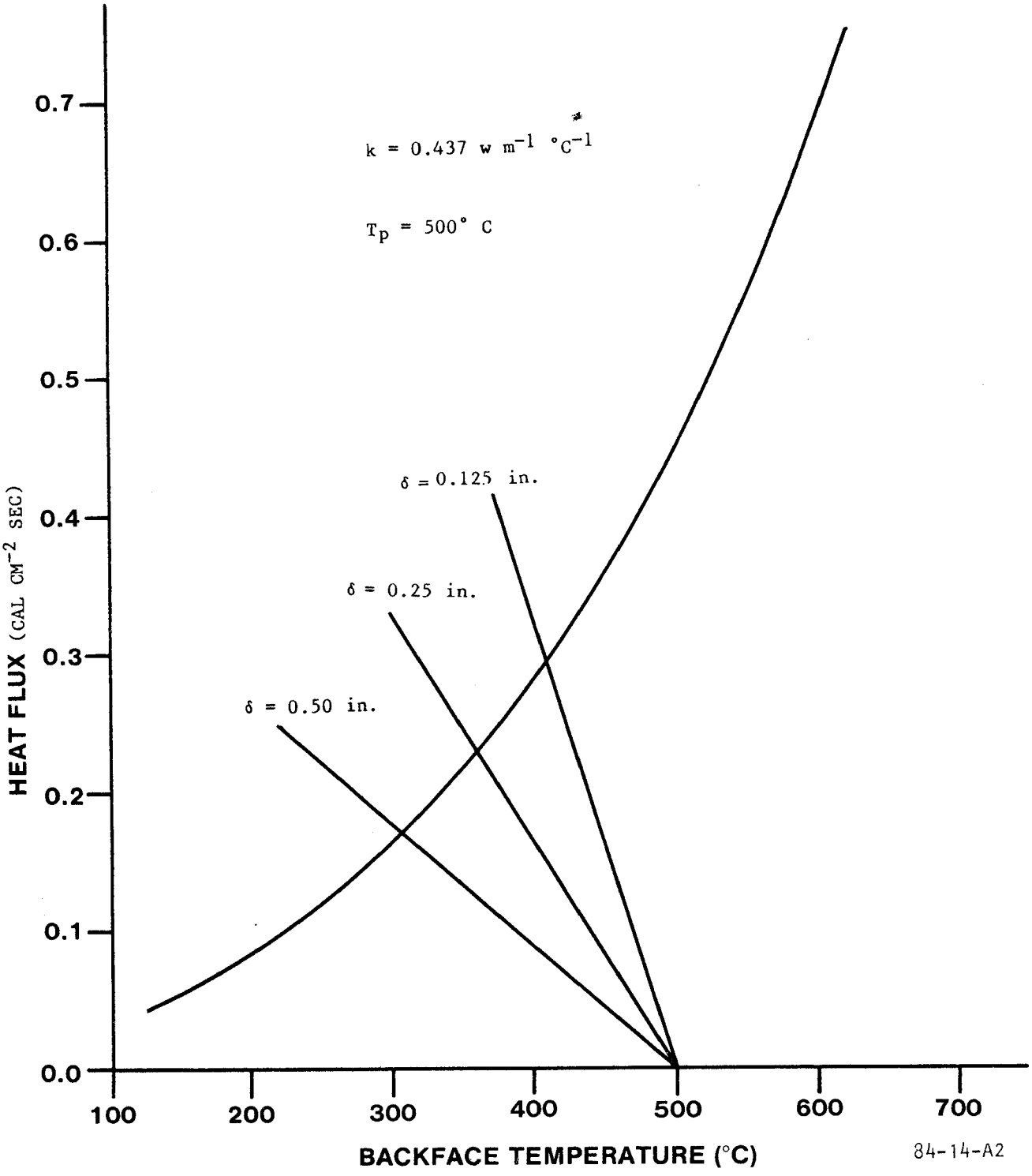

FIGURE A-2. EFFECT OF PANEL THICKNESS ON PANEL HEAT TRANSFER

APPENDIX B

THERMOGRAVIMETRIC ANALYSIS (TGA)

The polymer degradation temperatures listed in table 2 of the report are based on thermograms from the literature. The accuracy of ignition prediction from such data is dependent on the way the Thermogravimetric Analysis (TGA) is run, the type sample tested, and the interpretation. For instance, the TGA is usually run with the sample exposed to either air or nitrogen. Since ignitability of panels deals with a lean limit environment, TGA data with air flowing over the sample should be most appropriate. TGA devices also often use relatively low heating rates like 4 to 10° C per minute. Since the analysis for panel flammability is for slow ramp-type heating, the typical TGA heating rates should be appropriate. The TGA results are also affected by the following type sample effects: plasticizers in the resin, resin system ingredients, and differing panel plys. Vinylpolystyrlpyridine (VPSP) is a good example of these potential effects. Vinyl is added to this resin system to attain capabilities of curing at lower temperatures. The system also has bismaleimide as a major additional ingredient. Finally, TGA analysis of a VPSP facesheet would give a different result from a TGA analysis of a panel specimen including a Nomex core along with the VPSP.

The interpretation of the data also affords variations in the pyrolysis temperatures used in the flammability analysis. The mass loss midpoint is the simplest to extract from a TGA curve. However, even this approach requires that the raw TGA curve be available, or that the data be presented in that fashion. In the literature, the TGA data is actually reported often as the temperature of steepest weight loss or as a polymer degradation temperature derived from this slope. Figure B-1 shows two hypothetical curves for materials which might have the same mass loss mid-point denoted by m. Thus, T_m is the same for both. However, the temperature of steepest weight loss for material A differs from that for material B. That is, T_a is not the same as T_b. The polymer degradation temperature (PDT) is defined as the intersection of the steepest slope with the 100 percent line. Figure B-1 clearly shows that PDT_A is not the same as PDT_B. Because of the sensitivity of the heat flux needed for ignition to changes in the material decomposition temperature, this particular issue of data analysis becomes very important. Optimization of this panel flammability analysis would involve a thorough evaluation of which pyrolysis temperature most effectively correlated with experiments on panel flammability.

The remaining figures of this appendix present the TGA curves actually employed in developing table 2 of this report.

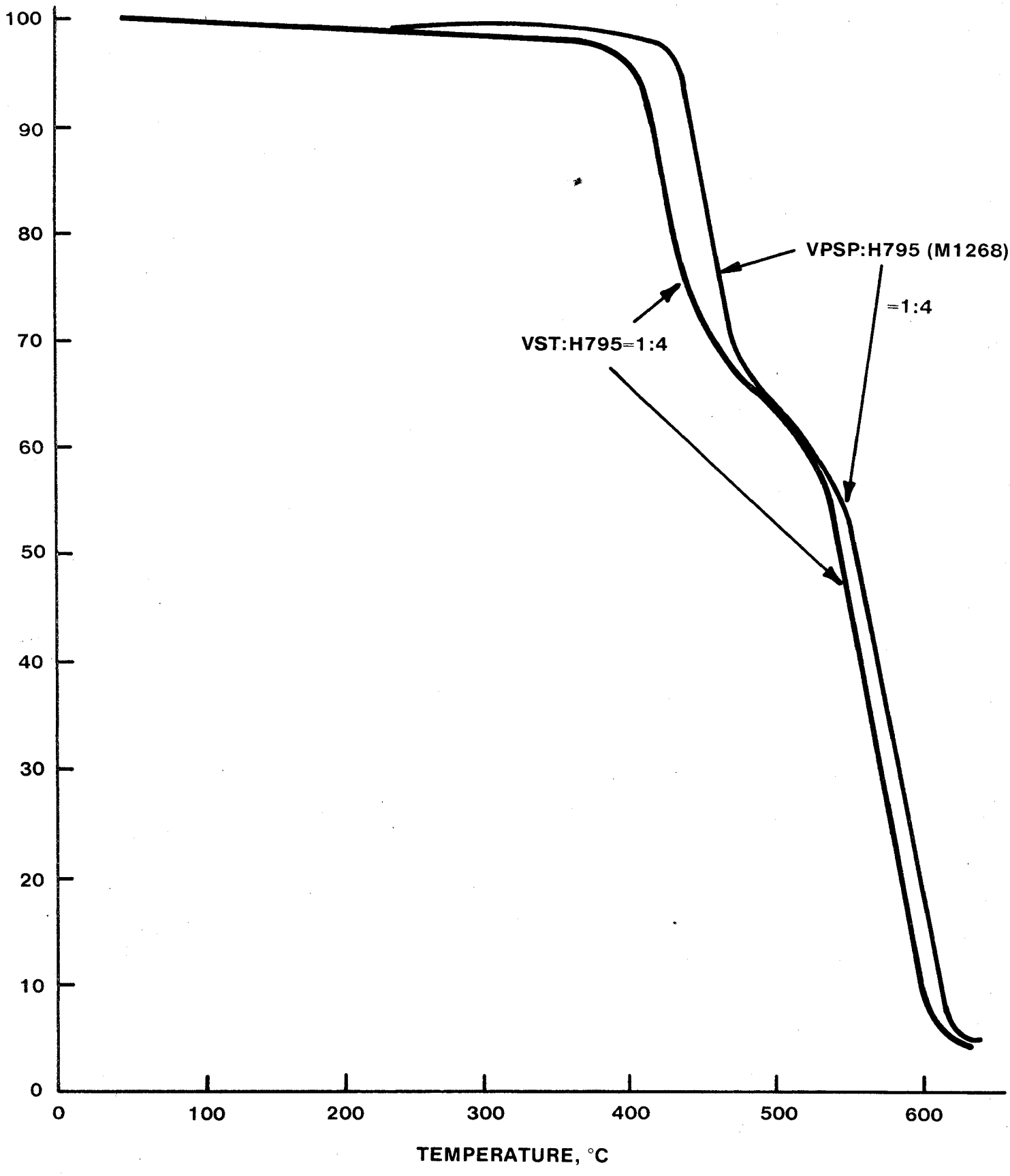

FIGURE B-1. TYPICAL THERMOGRAVIMETRIC ANALYSIS OF VINYLSTYRYLPYRIDINE MODIFIED BISMALEIMIDE IN AIR (10°C/min) (TAKEN FROM REFERENCE 12)

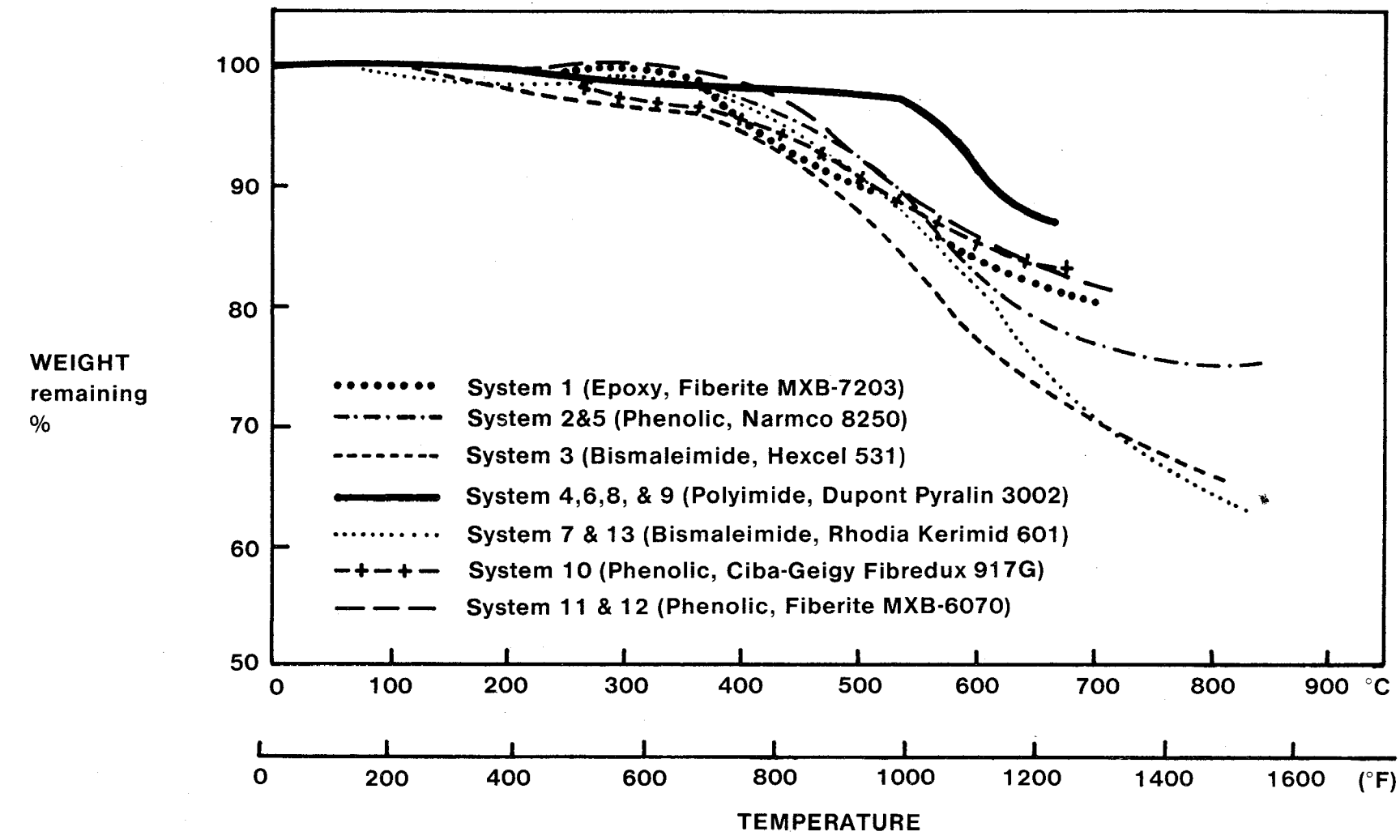

FIGURE B-2. THERMOGRAVIMETRIC ANALYSIS - FACE SHEETS - TASK 2
(TAKEN FROM REFERENCE 10)

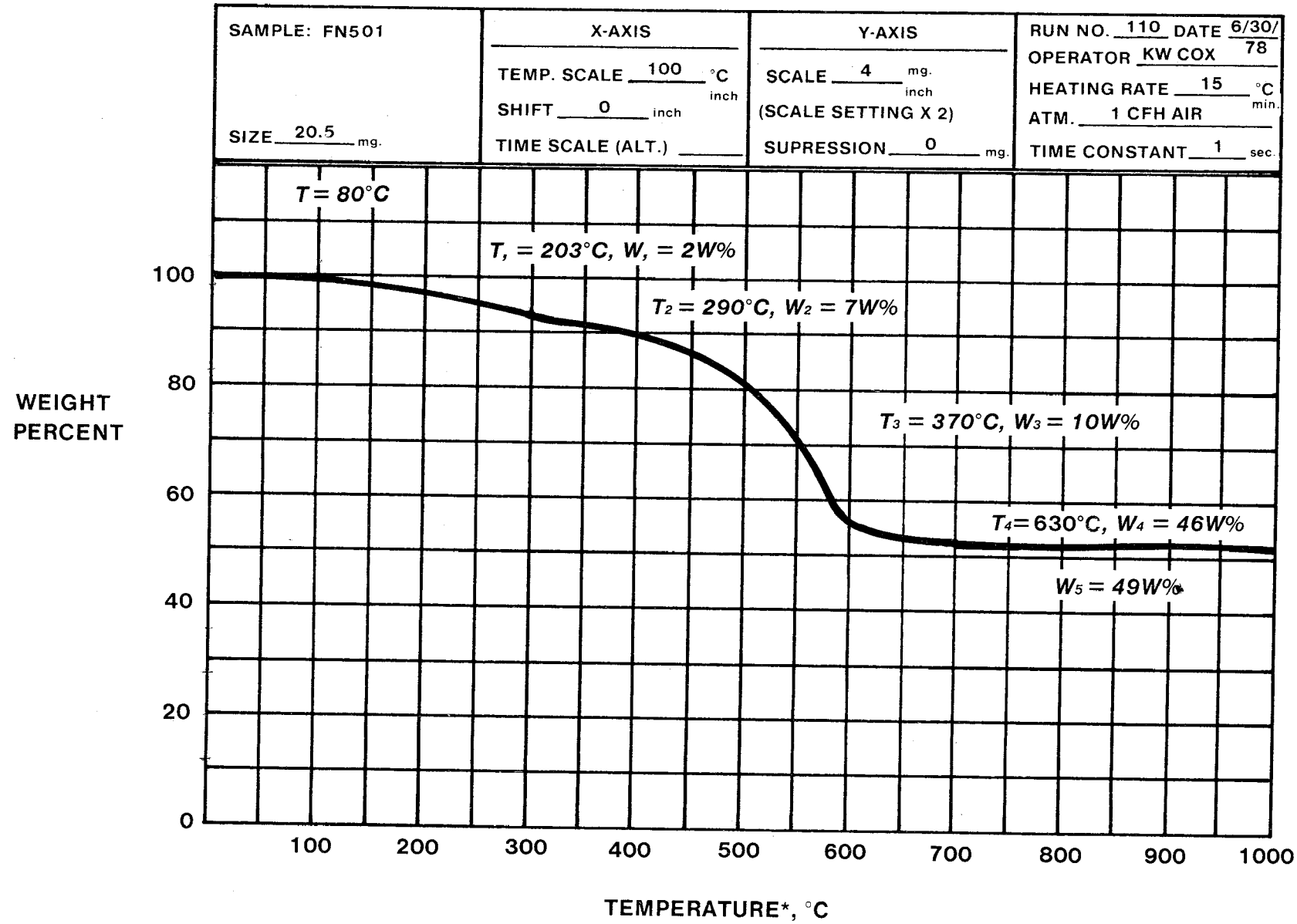

FIGURE B-3. THERMOGRAM F501 (CIBA GEIGY FIBERDUX 917) PHENOLIC (TAKEN FROM REFERENCE 11)

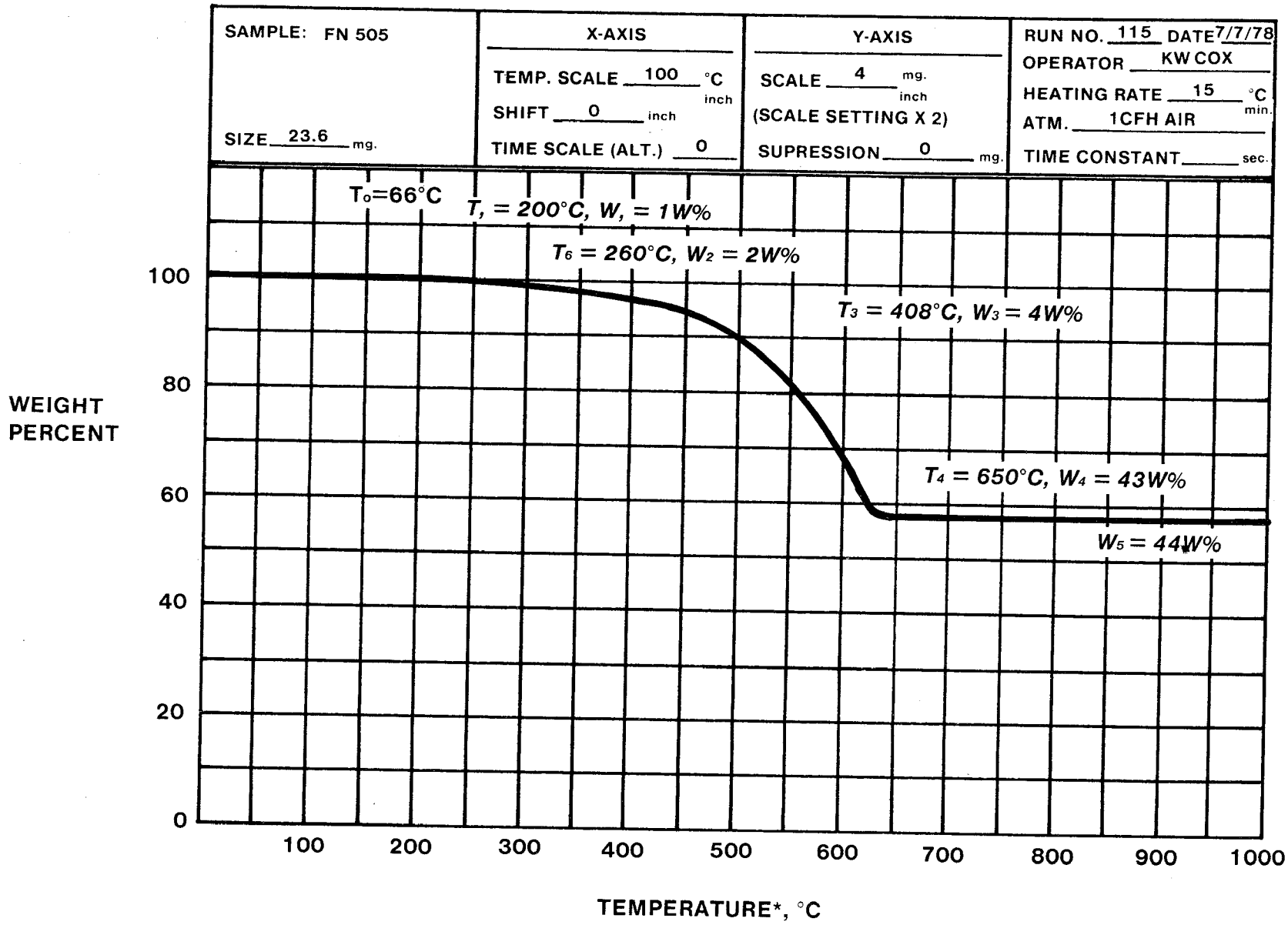

FIGURE B-4. THERMOGRAM F505 (NARMCO 8250) PHENOLIC (TAKEN FROM REFRENCE 11)

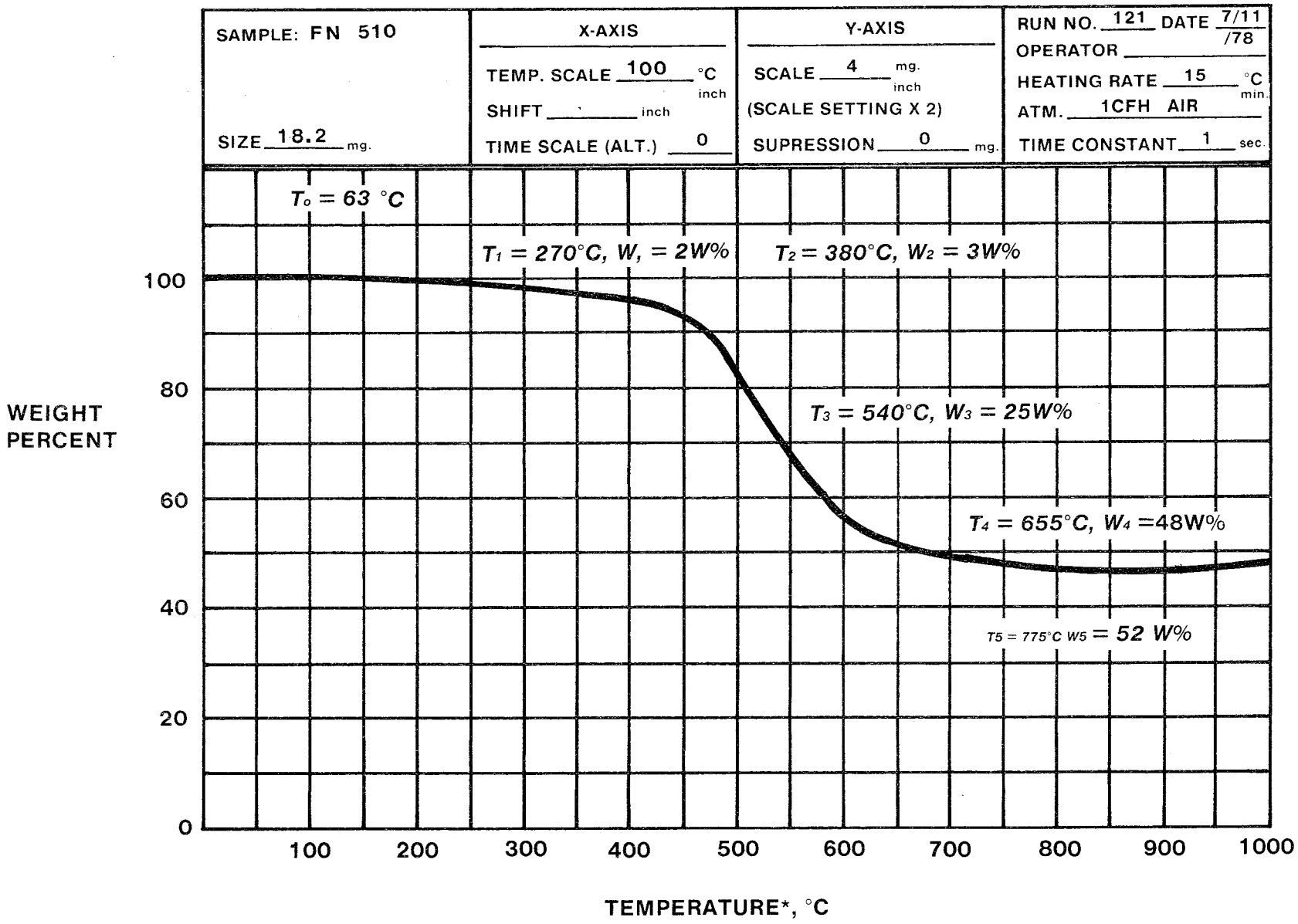

FIGURE B-5. THERMOGRAM F510 (FIBERITE MXT 6032) PHENOLIC (TAKEN FROM REFERENCE 11)

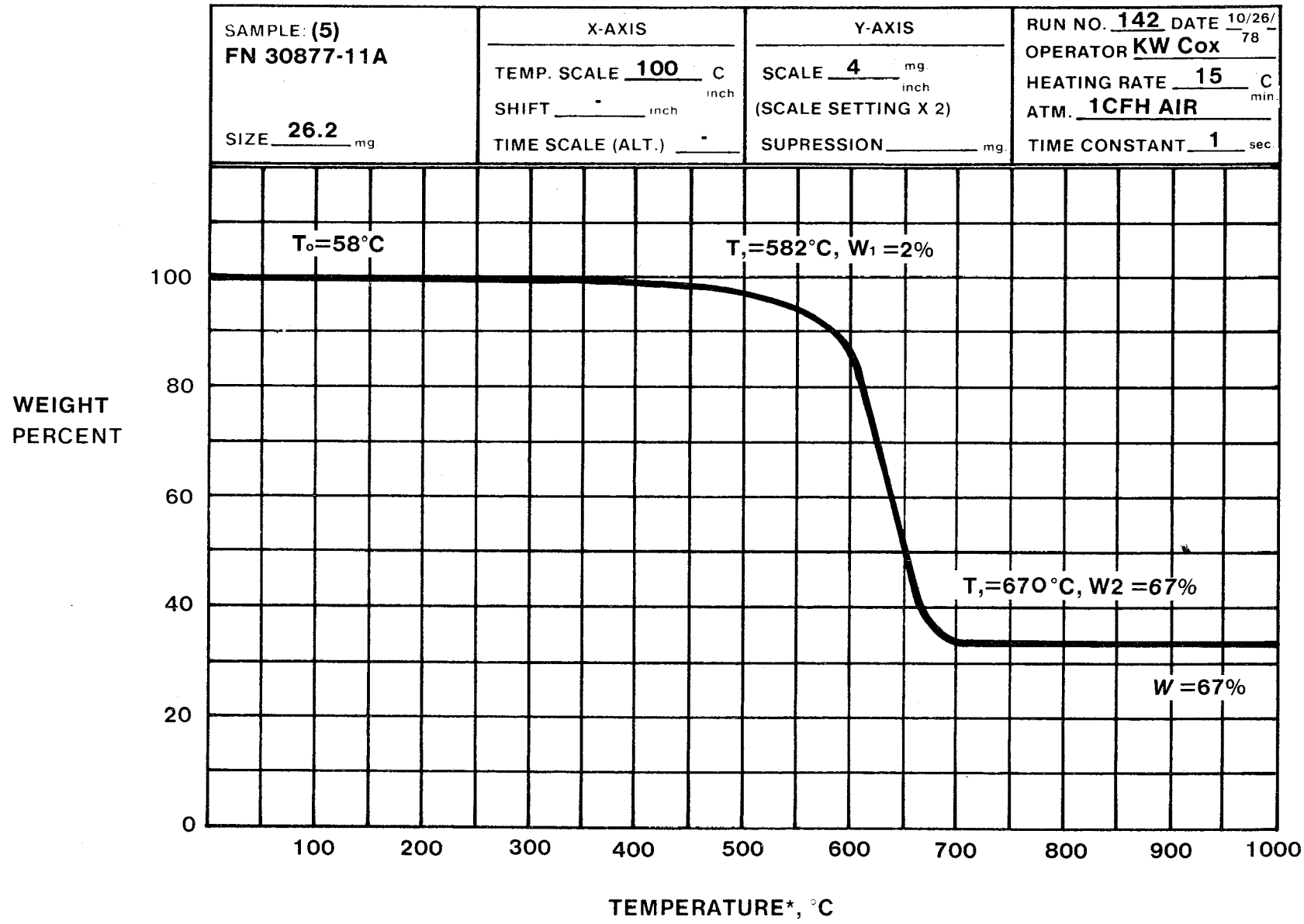

FIGURE B-6. THERMOGRAM FN308/7-11A (POLYIMIDE/GLASS) (TAKEN FROM REFERENCE 11)